Formation of TiB$_2$–TiC composites by reactive sintering

Hong Zhao, Yi-Bing Cheng*

Department of Materials Engineering, Monash University, Melbourne, VIC 3168, Australia

Abstract

TiB$_2$ and TiC are covalent compounds and possess excellent hardness and corrosion resistance. It is very difficult to densify these materials using conventional sintering techniques. In this study, reactive sintering was used to simultaneously synthesise and densify TiB$_2$–TiC composites. Solid state diffusion was the chief mechanism involved in the sintering process. Intermediate boride phases were formed and their amount and stability were strongly dependent on the sintering temperature and time. It was found that the chemical reaction between the starting Ti metal and B$_4$C particles could be complete after sintering at ~1500°C for 1 h, producing a TiB$_2$–TiC ceramic composite. © 1999 Elsevier Science Limited and Techna S.r.l. All rights reserved.

Keywords: D. Borides; D. Carbides; Reactive sintering; Composites

1. Introduction

Boride ceramics have some special properties, such as high melting points, high hardness, high electrical conductivity and excellent resistance to the attack by some molten metals. The high conductivity of the borides makes them easier and more economical to be machined after sintering by electrical discharge machining technique [1]. The boride materials, therefore, have great potential to be used as refractories and electrodes for metallurgical industries, particularly for the aluminium industry [2–5]. The composites that combine boride and carbide offer an attractive combination of excellent mechanical and electrical properties and corrosion resistance, particularly at relatively high temperatures and/or in corrosive environments [6–8].

The application of TiB$_2$ based ceramics is often limited by the high costs associated with the materials because of the expensive starting materials, such as TiB$_2$ powder, and the often used high temperature pressure sintering technique. Reactive sintering is a technique in which both the chemical reactions of the starting materials and densification occur in a single firing step [9]. This technique can be economical due to cheap starting powders and relatively low sintering temperature, and it also leads to the possibility of densifying the materials with less additives or even without additives at all. Reactive sintering has shown its usefulness in producing TiB$_2$-based ceramic composites with a compacted mixture of reactant powders. Barsoum et al. [10,11] employed the transient plastic phase processing (TPPP) technique in which Ti metal was seen as a transient plastic phase. By this way, TiC–TiB$_2$ and TiC$_{0.6}$–TiB$_2$–Ti$_3$B$_4$ composites were hot-pressed at a relatively low sintering temperature (1600°C) using starting powder mixtures of Ti/B$_4$C and TiC$_{0.5}$/TiB$_2$, respectively. Different intermediate phases were identified in their work during sintering when starting powders were different. Ti$_3$B$_4$ grains with platelet morphology were developed in the TiC$_{0.6}$–TiB$_2$–Ti$_3$B$_4$ composite, as a result of the conversion of an intermediate phase of TiB, which contribute to its high strength and toughness. The procedure of reactive hot pressing for the TiC$_{0.6}$–TiB$_2$–Ti$_3$B$_4$ composite was extensively studied, but no such detailed explanation for the TiC–TiB$_2$ system was given. Zhang et al. [12,13] explored composites TiB$_2$–SiC and TiB$_2$–TiC–SiC rather than TiB$_2$–TiC using hot-pressing from a powder mixture of TiH$_2$, Si and B$_4$C. The hot-pressing technique was employed in those works to achieve materials with relatively high density.

The present work investigates the reaction sintering process that leads to the formation of TiB$_2$–TiC composites from a starting powder mixture of Ti and B$_4$C. All the materials were produced via pressureless sintering. The basic reaction involved in the materials formation is:

$$3Ti + B_4C = 2TiB_2 + TiC \qquad (1)$$

---

* Corresponding author.

The understanding of intermediate phases and microstructures occurring at different stages is critical for the development of desired ceramic composites formed by reaction sintering. This work, therefore, concentrates on the study of the reaction mechanisms and the microstructural development of these materials at various firing conditions based on XRD and SEM observations as well as thermodynamical calculation.

2. Experimental procedures

Based on the reaction Eq. (1), the stoichiometric starting powders of Ti (Cerac, −325 mesh) and B_4C (Fluka, −325 mesh) were mixed in ethanol using Si_3N_4 balls as media for 24 h and then dried at 80°C. The dried powder mixtures were uniaxially pressed into pellets of 25 mm in diameter and 10 mm in height and followed by cold isostatic pressing at 200 MPa. The pellets were placed into a graphite crucible and pressureless sintered in a graphite furnace in an argon atmosphere. In order to investigate the reaction mechanisms, the samples were heated at a fast rate of 45°C/min to various temperatures and cooled in the furnace by turning off power to achieve rapid cooling. The natural cooling rate of the furnace is about 40°C/min from 1800 to 1500°C and about 25°C/min from 1500 to 1000°C. Two holding times, 5 and 60 min, were adopted, respectively. To study the chemical reaction on heating, the 5 min holding time is to ensure that the temperature inside the crucible has just reached the designed level but there is insufficient time for further chemical reaction. Experiments holding for 60 min at a temperature serve the purpose of studying the influence of dwell time on the reaction sintering.

Bulk densities of the as-sintered samples were determined using the mercury immersion technique. In order to reveal the bulk composition of the fired samples, the surfaces of the as-sintered samples were removed for more than 0.5 mm, and then subjected to phase identification using a Rigaku Geigerflex X-ray diffractometer. The microstructures were observed using a Jeol 840A scanning electron microscope and attached energy dispersive X-ray spectrometer (EDXS). Due to the conducting nature of the samples, no conductive surface coating was required prior to the SEM observation.

3. Results and discussion

Standard free energies of the basic reaction [Eq. (1)] as well as other possible reactions that may occur in the system have been calculated based on the thermodynamic data obtained from Refs. [14] and [15] (Fig. 1). It can be seen that the basic reaction [Eq. (1)] has a negative free energy and its driving force increases with

temperature, indicating that its products would become the dominant phases at high temperatures.

The reaction sequence of Eq. (1) was determined from the XRD results of the samples fired at temperatures from 1000 to 1650°C for 5 and 60 min holding times, respectively (Table 1). In the samples fired for 5 min, the initial products were identified at 1100°C, but the reaction was insignificant until the temperature reached 1300°C. An intermediate phase Ti_3B_4 existed in a wide range of temperature from 1100 to 1500°C, but presented in a weak or very weak intensity in XRD spectra. More intense reactions took place from 1300°C upwards and another intermediate phase TiB became notable above 1400°C. All the intermediate phases, however, disappeared when temperature rose above 1500°C. The reaction completed when temperature was above 1650°C even only for a 5 min holding time.
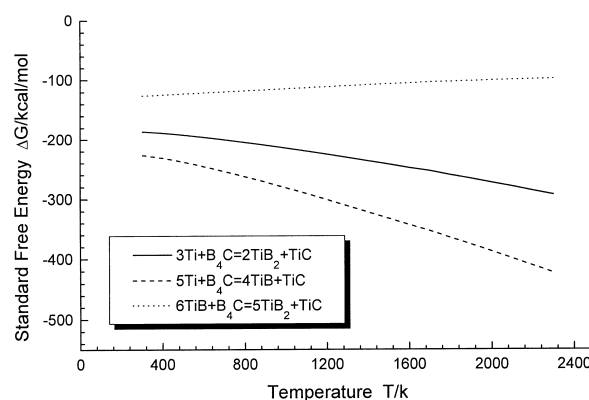

Fig. 1. Standard Gibbs free energy calculated for reaction $3Ti + B_4C = 2TiB_2 + TiC$ and its intermediate reactions.

Table 1
XRD results of the reaction [Eq. (1)] fired at different temperatures with different dwell times

Temperature (°C)	Dwell time (min)	Reactants		Transients		Products	
		Ti	B_4C	Ti_3B_4	TiB	TiB_2	TiC
1000	5	vs	S	–	–	–	–
1100	5	vs	S	vw	–	–	vw
1200	5	vs	S	w	–	vw	w
1300	5	s	S	w	vw	w	m
1400	5	m	M	vw	–	m	m
1500	5	–	W	w	m	s	s
1650	5	–	–	–	–	vs	s
1750	5	–	–	–	–	vs	s
1150	60	s	M	w	w	w	m
1200	60	m	M	w	vs	m	m
1300	60	vw	W	vw	m	m	s
1400	60	–	w	–	w	s	s
1500	60	–	–	–	–	vs	s

Note: X-ray intensity: vw, very weak; w, weak; m, medium; s, strong; vs, very strong.
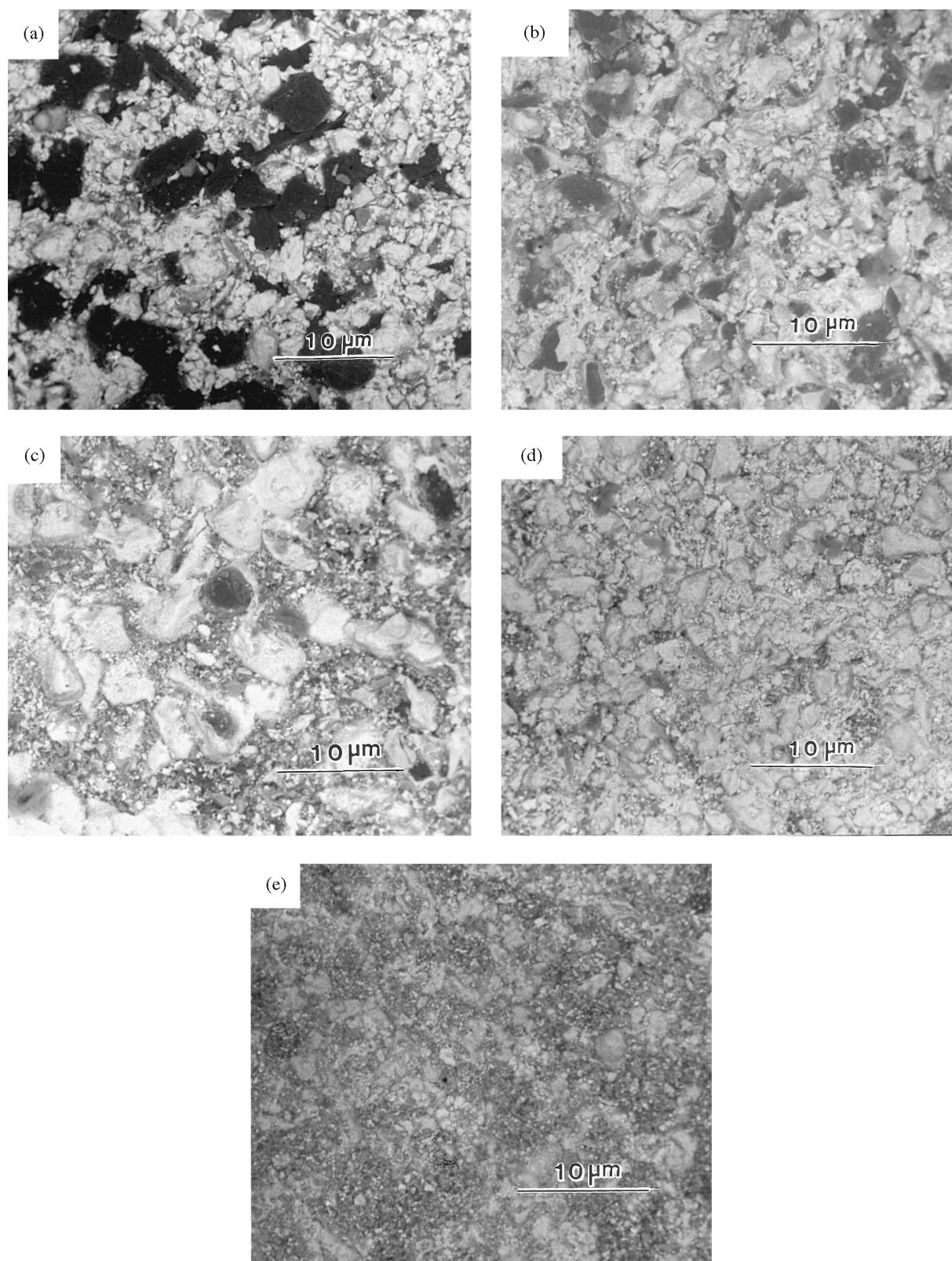
Fig. 2. Back scatter images of reaction $3Ti + B_4C = 2TiB_2 + TiC$ fired for a 5 min dwell time at (a) 900°C, (b) 1300°C, (c) 1500°C, (d) 1650°C and (e) 1750°C.

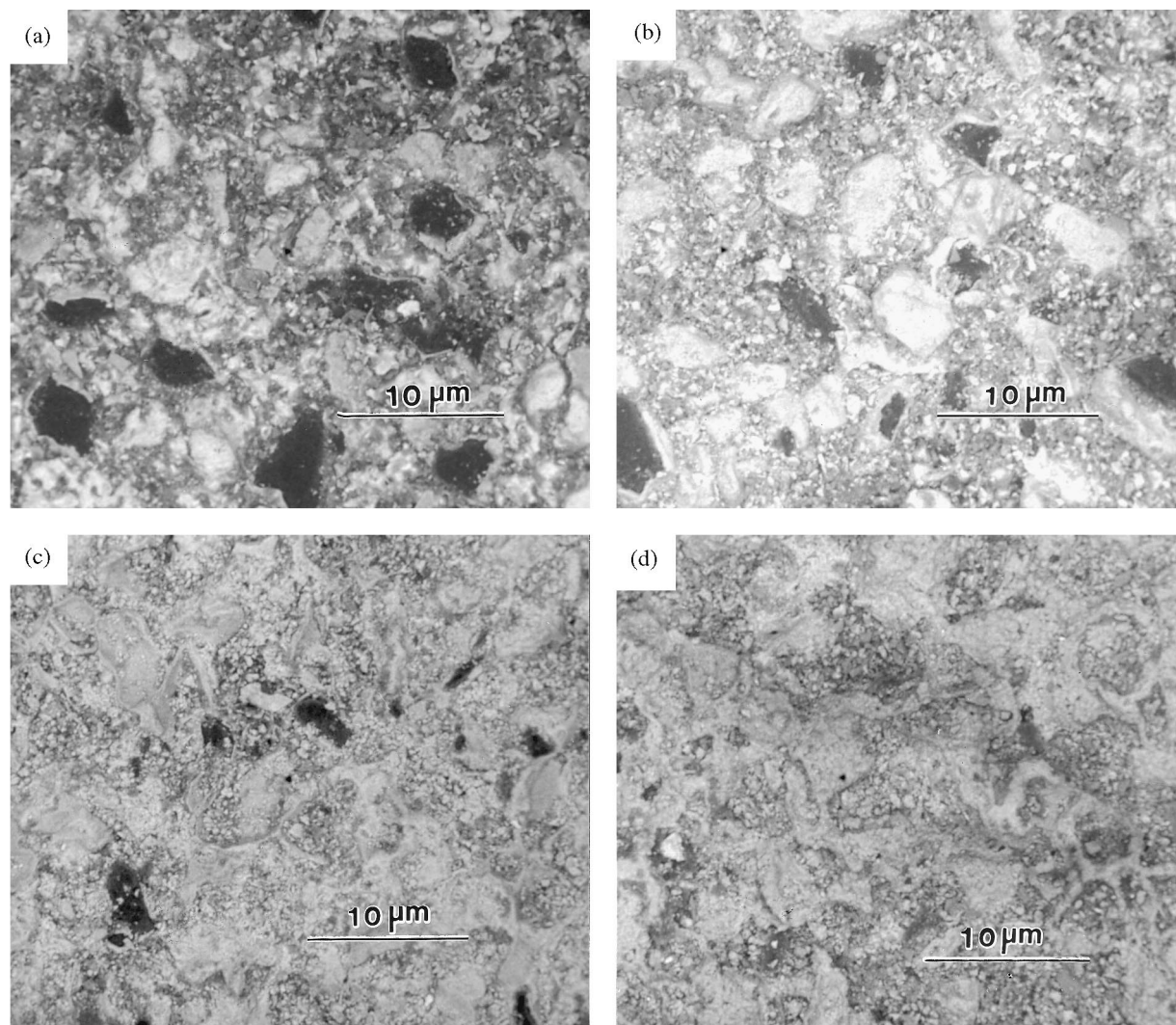Fig. 3. Back scatter images of reaction $3Ti + B_4C = 2TiB_2 + TiC$ fired for a 60 min dwell time at (a) 1200°C, (b) 1300°C, (c) 1400°C and (d) 1500°C.

Firing time has a very significant effect on the chemical reactions of the system. Although same intermediate and final crystalline phases were obtained, different features were seen in samples sintered for 60 min comparing to those for 5 min (Table 1). It was found that to achieve the same extent of reaction the temperature was significantly lowered for samples fired for a longer time. For instance, the temperature required for the intermediate phase TiB to appear in a medium or strong intensity was 1200°C in the sample fired for 60 min but 1500°C in that fired for only 5 min. This indicates the importance of diffusion in the reactions. Meanwhile, by extending the sintering time from 5 to 60 min, the reaction completing temperature was reduced by about 150°C.

Microstructure observation was in agreement with the XRD identification. Figs. 2 and 3 showed the back scatter images of samples fired at various temperatures for 5 and 60 min, respectively, where dark areas represented the starting B_4C particles and bright areas Ti,

TiC, TiB_2, Ti_3B_4 and TiB due to the existence of Ti element in these phases. Reaction between B_4C and Ti was apparent in both the short- and long-firing samples. With increasing temperature, B_4C particles became smaller and were gradually consumed. The highly contrasted dark B_4C phase disappeared from the samples sintered at 1650°C for 5 min (Fig. 2d) and 1500°C for 60 min (Fig. 3d), respectively, indicating the completion of the reaction. The product particles are in a relatively large size (~ 5 µm) when fired at 1500°C for 5 min, but interestingly, the particle size of the final resultants at 1750°C (Fig. 2e) was actually refined, even smaller than those of the starting reactants (Fig. 2a). It seemed that the rapid increase in temperature above 1500°C facilitated fast reaction between starting materials and the intermediate phases to form fine TiB_2 and TiC particles, but it gave little time for grain growth.

Intermediate products TiB and Ti_3B_4 were detected from XRD in both series of samples (Table 1). It was very difficult to distinguish these Ti-containing phases
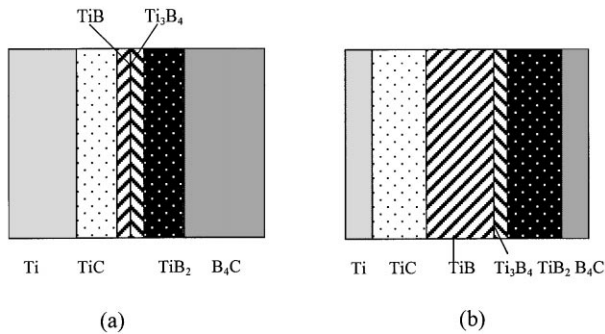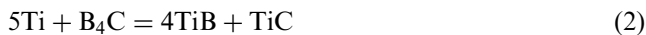
Fig. 4. Schematic diagrams of reaction $3Ti + B_4C = 2TiB_2 + TiC$ at (a) low temperatures and (b) high temperatures. Because diffusion of boron was relatively slow in this system, transit phases formed due to the compositional gradient at the interface between the starting Ti and B_4C particles.

by their microstructures as very little contrast in the back scattered SEM images existed between them and the EDXS facility used in this work was insensitive to boron and carbon elements. TiB appeared with a medium or even strong XRD intensity shortly before the completion of the reaction, while only weak or very weak Ti_3B_4 peaks were detected in this reaction procedure. Based on these results and thermodynamic calculation (Fig. 1), the following two reaction paths are suggested for the transition from the starting powders to the final TiB_2–TiC composites:

Path I

$$5Ti + B_4C = 4TiB + TiC \tag{2}$$

$$16TiB + B_4C = 5Ti_3B_4 + TiC \tag{3}$$

$$3Ti_3B_4 + B_4C = 8TiB_2 + TiC \tag{4}$$

Path II

$$5Ti + B_4C = 4TiB + TiC \tag{2}$$

$$6TiB + B_4C = 5TiB_2 + TiC \tag{5}$$

Both reaction paths lead to the same final products and they occur simultaneously during sintering. According to the proposed reaction paths, the TiC phase should form before TiB_2, which is in good agreement with the XRD results (Table 1), although the overall proportion of the former phase in the final products is less than the latter.

If the reaction relied on mutual diffusion of carbon and boron into titanium and vice versa, the reaction processes could be schematically represented in Fig. 4. At the interface between Ti and B_4C particles, initial atomic diffusion facilitated Ti-containing compounds to form, following the reaction path 1. The diffusivity of carbon was significantly greater than that of boron [16].

Thus, carbon readily combined with titanium to yield TiC at all sintering temperatures and produced no other carbon-containing phase. But a concentration gradient of boron existed along the diffusion path between Ti and B_4C particles, resulting in the formation of TiB, Ti_3B_4 and TiB_2 phases depending on the ratio of Ti:B. At higher temperatures, reaction path II was most likely to become dominant without the transit phase Ti_3B_4 due to rapid diffusion, leading to a large amount of intermediate phase TiB. The microstructural feature for such a compositional gradient (TiB, Ti_3B_4 and TiB_2) presented a core-rim structure of grains in the samples fired at 1300 and 1500°C for 5 min, with the transit phases at the rim surrounding the core of the starting Ti and B_4C particles (Fig. 2b,c). Increasing temperature and time accelerated diffusion and promoted TiB to convert into TiB_2, leading to a much more homogeneous microstructure (Fig. 2e).

4. Summary

TiB_2–TiC composites have been formed using reactive sintering of Ti metal and B_4C powders. The chemical reaction of the system relies primarily on solid state diffusion between B, C and Ti and is critically affected by sintering temperature and time. A relatively slow diffusion of B atom resulted in a series of intermediate boride phases formed at the interfaces between the starting Ti and B_4C particles. Nevertheless, a complete reaction can be achieved at 1500°C for 1 h, offering potential to produce TiB_2–TiC composites at commercially viable conditions.

References

[1] J. Matsushita, T. Suzuki, A. Sano, Wire electrical discharge machining of TiB$_2$ Composite, J. Ceram. Soc. Jap., 100 (1992) 219–222.
[2] J.B. Todd, Energy reduction in Hall–Heorult cell with conventional and special electrodes, J. Met. 33 (1981) 42–45.
[3] C.J. McMinn, A review of RHM cathode development. in: E.R. Cutshall (Ed.), Light Metals, TMS, Pennsylvania, USA, 1992, pp. 419–425.
[4] K. Billehaug, H.A. Oy, Inert cathodes for aluminium electrolysis in Hall–Heroult cells (I), Aluminium 56 (1980) 642–648.
[5] K. Billehaug, H.A. Oy, Inert cathodes for aluminium electrolysis in Hall–Heroult cells (II), Aluminium 56 (1980) 713–718.
[6] M.A. Janney, Mechanical properties and oxidation behaviour of a hot-pressed SiC–15-vol%-TiB$_2$ Composite, Am. Ceram. Soc. Bull. 66 (1987) 322–324.

[7] C.H. McMurty, W.D.G. Boecker, S.G. Seshadri, J.S. Zanghi, J.E.A. Garnier, Microstructure and material properties of SiC–TiB$_2$ particulate composites, Am. Ceram. Soc. Bull. 66 (1987) 325–329.

[8] M.G. Jenkins, J.A. Salem, S.G. Seshadri, Fracture resistance of a TiB$_2$ particle/SiC matrix composite at elevated temperature, J. Compos. Mater. 23 (1989) 77–91.

[9] F. Hong, M.H. Lewis, Ceramic–matrix composites via in-situ reaction sintering, Ceram. Eng. Sci. Proc. 14 (1993) 699–706.

[10] M.W. Barsoum, B. Houng, Transient plastic phase processing of titanium–boron–carbon composites, J. Am. Ceram. Soc. 76 (1993) 1445–1451.

[11] D. Brodkin, S. Kalidindi, M. Barsoum, A. Zavaliangos, Microstructural evaluation during transient plastic processing of titanium carbide–titanium boride composites, J. Am. Ceram. Soc. 79 (1996) 1945–1952.

[12] G.J. Zhang, Z.Z. Jin, X.M. Yue, Reaction synthesis of TiB$_2$–SiC composites from TiH$_2$–Si–B$_4$C, Mater. Lett. 25 (1995) 97–100.

[13] G.J. Zhang, X.M. Yue, Z.Z. Jin, Preparation and microstructure of TiB$_2$–TiC–SiC platelet-reinforced ceramics by reactive hot-pressing, J. Eur. Ceram. Soc. 16 (1996) 1145–1148.

[14] I. Brarin, O. Knacke, Thermochemical Properties of Inorganic Substances, Springer, Berlin, Germany, 1973.

[15] I. Brarin, O. Knacke, Thermochemical Properties of Inorganic Substances—Supplement, Springer, Berlin, Germany, 1977.

[16] A.L. Laskar, J.L. Bocquet, G. Brebec, C. Monty, Diffusion in Materials, Kluwer, Dordrecht, The Netherlands, 1990.